[26] D.V. Morrissey, J.A. Lockridge, L. Shaw, K. Blanchard, K. Jensen, W. Breen, K. Hartsough, L. Machemer, S. Radka, V. Jadhav, N. Vaish, S. Zinnen, C. Vargeese, K. Bowman, C.S. Shaffer, L.B. Jeffs, A. Judge, I. Maclachlan, B. Polisky, Potent and persistent in vivo anti-HBV activity of chemically modified siRNAs, Nat. Biotechnol. 23 (2005) 1002–1007.

[27] A.D. Judge, V. Sood, J.R. Shaw, D. Fang, K. Mcclintock, I. Maclachlan, Sequence-dependent stimulation of the mammalian innate immune response by synthetic siRNA, Nat. Biotechnol. 23 (2005) 457–462.

[28] T.S. Zimmeemamm, A.C. Lee, A. Akinc, B. Bramlage, D. Bumcrot, M.N. Fedoruk, J. Harborth, J.A. Heyes, L.B. Jeffs, M. John, A.D. Judge, K. Lam, K. McClintock, L.V. Nechev, L.R. Palmer, T. Racie, I. Rohl, S. Seiffert, S. Shanmugam, V. Sood, J. Soutschek, I. Toudjarska, A.J. Wheat, E. Yaworski, W. Zedalis, V. Koteliansky, M. Manoharan, H.P. Vornloche, I. MacLachlan, RNAi-mediated gene silencing in non-human primates, Nature 441 (2006) 111–114.

[29] M. Schlee, V. Hornung, G. Hartmann, siRNA and isRNA: two edges of one sword, Mol. Ther. 14 (2006) 463–470.

[30] R.E. Lanford, D. Chavez, B. Guerra, J.Y.N. Lau, Z. Hong, K.M. Brasky, B. Beames, Ribavirin induces error-prone replication of GB virus B in primary tamarin hepatocytes, J. Virol. 75 (2001) 8074–8081.

[31] K. Li, Z. Chen, N. Kato, M. Gale Jr., S.M. Lemon, Distinct poly(I-C) and virus-activated signaling pathways leading to interferon-beta production in hepatocytes, J. Biol. Chem. 280 (2005) 16739–16747.

特集

獣医師に求められるコンプライアンス　－法規制，知らなかったでは済まされない－

医学実験用霊長類を用いた病原体感染実験施設の管理運営におけるコンプライアンスとバイオセーフティ

明里宏文

要　約

近年の新興再興感染症の拡大は我が国のみならず世界的にも危急の問題となっており，この克服に向けた基盤的研究が精力的に国内外で進められている。特にその原因微生物による疾患の病態解明や予防治療法開発において，医学実験用霊長類を用いた動物モデル研究は不可欠となっている。本項では，このような研究を推進する上で必要な病原体感染実験施設におけるコンプライアンスについて，主にバイオセーフティの観点から概説したい。

序　論

感染症研究における霊長類を用いた動物モデルの意義

20世紀初頭まで人類全体の脅威であった「伝染病」は，医学研究の進歩，特にワクチン開発および抗生物質の発見によりその多くが致死的疾病から免れることができるようになり，もはや脅威ではなくなったかに見えた。しかし，こうした予想に反して，現在では新たな感染症の脅威 - 新興再興感染症に人類は直面している。すなわち交通手段の高速化・グローバル化，一方では輸血や注射等非衛生的条件下における様々な医療行為等は，エンデミックな病原微生物の世界的規模での拡散を可能とした。AIDSはこの代表例としてあげられる。当初AIDSはアフリカ一地方の風土病であったものが1970～1980年代に欧米に拡散し，現在もアジア・アフリカ諸国において感染者が増大の一途を辿っている。近年では，C型肝炎，プリオン病（牛の海綿状脳症，人では変異型クロイツフェルト・ヤコブ病），SARS（重症呼吸器症候群），鳥インフルエンザなど枚挙にいとまがない。

このような新興再興感染症による脅威に立ち向かい制圧していくにあたっては，その原因微生物による疾患の病態やその発症機序を分子レベルで解明し，その研究成果を基に新規治療薬や有効なワクチンを開発していく事が期待される。このような基礎・応用研究を推進し，臨床現場に反映させるためには，動物モデルを用いた実験感染系の確立およびこれを用いた候補薬等の安全性・有効性評価に関する前臨床試験（いわゆるトランスレーショナルリサーチ）が不可欠である。

こうした動物モデル研究では通常マウスやラットなどの小動物が第一選択となる。ところが新興再興感染症における研究の場合，実際には病原体がこうした小動物に感染・発症しない場合が多く見られる。他方，人にもっとも近縁な動物であるサル類をモデル動物として用いることにより，原因病原体に感染し人で生じるような病態を再現できる場合が多く認められる。このため新興再興感染症研究における霊長類モデルの重要性は近年非常に高まっているのが実情である。こうした社会的要請から，独立行政法人医薬基盤研究所・霊長類医科学研究センターでは，実験用サル類を用いた各種感染症の動物モデル研究を実施している。これまでに，AIDS研究を始めとしてプリオン病，結核，ウイルス肝炎，マラリア，デング熱など様々な感染症に関する重要な知見が得られている。

Hirofumi AKARI：独立行政法人医薬基盤研究所 霊長類医科学研究センター・疾患制御研究室（〒305-0843 茨城県つくば市八幡台1-1）

当センター着任後，本来の研究テーマであるウイルス感染症モデル開発およびその基盤的研究を進める傍ら，霊長類感染症実験施設の管理運営という二足の草鞋を穿くことになりました。当初は様々な困難に直面しましたが，多くの方々からのサポートのおかげで，ようやくある程度の基礎ができつつあるところです。

実験用霊長類を用いる感染症モデル研究実施におけるコンプライアンス

感染症モデル研究（もちろんそれ以外の医科学研究も含めて）において実験用霊長類を用いるに当たっては，その特殊性から様々なコンプライアンスが求められ，さらに多くのリスクを伴うことから，その研究実施に当たってはサル類以外の選択肢がない，すなわちサル類を用いること以外での代替法がない場合で，かつその実施によりリスクを上回る重要性や成果が期待される場合に限られなければならない。関連する主なコンプライアンスを以下に示す。

■サル取扱いに関するコンプライアンス

①動物愛護管理法：特にサル類を医科学実験に用いる際には，動物福祉面や倫理上の観点から充分な配慮と厳密な規制が必要

②ワシントン条約（CITES）：サルおよびサル材料の輸出入制限

■遺伝子組換え微生物の取扱に関するコンプライアンス

①カルタヘナ議定書：生物多様性に関する国際条約に基づき制定

②遺伝子組換え生物等の使用規制法：遺伝子組換え微生物等の取扱い

■病原体に関するコンプライアンス

①改正感染症法：バイオテロ対策

②バイオセーフティ管理：病原体取扱における安全管理

■薬物，化学物質の取扱に関するコンプライアンス

①獣医師法，薬事法：動物医薬品の安全管理

②麻薬取締法：特に昨年度からの塩酸ケタミン麻薬指定

ここでは本題である医学実験用霊長類におけるバイオーセーフティ管理について解説する。それ以外のコンプライアンスについては他項の総説をご参照願いたい。

実験用霊長類を用いる感染症モデル研究実施におけるバイオハザードの可能性

感染症モデル動物としてサル類を用いるに当たっては，その人との近縁性からバイオハザード（生物学的災害）によるリスクを充分に認識しておくことが肝要である。

1）病原体取扱者（病原体研究者，動物作業従事者，獣医師，施設管理者を含む）のバイオハザード

①研究目的のためサル類に感染させた病原微生物に，誤って人が暴露することにより感染・発症する可能性が考えられる。本来，人に病原性を有する微生物でありバイオハザードのリスクは高いが，予め各実験ごとに事故時の対応法，治療法などのマニュアルを作成しておくことでリスク低減を図ることが可能である（後述）。

②サル類はその人との類似性から，サル・人共に病原性を有するいわゆる人獣共通感染症（ズーノーシス）の原因微生物に感染している可能性が考えられる。特にズーノーシスとして留意すべき病原体としてBウイルスが挙げられる。Bウイルスについては，以下のウェブサイトに詳述されている。

http://wwwsoc.nii.ac.jp/jsvs/05_byouki/infect/07-B-virus.html

http://idsc.nih.go.jp/idwr/kansen/k00-g45/k00_41/k00_41.html

概　説：Bウイルスはαヘルペスウイルスに分類され，アジア産マカクに広く感染している。ただしこれまでに人への病原性が報告されているものはアカゲザル由来ウイルスのみである。通常は神経節に潜伏感染し，実験操作や輸送によるストレスや免疫抑制により再活性化し唾液や排泄物中にウイルスを排出する。これが人への感染源となる。サルには口腔内潰瘍などの病原性を示す程度だが，人への感染は風邪様症状の後，時として神経症状を呈し死の転帰を辿る。これまでに40例ほどの死亡例が報告されている。神経症状発症までの抗ヘルペス薬服用が有効である。

③研究に供したサル個体が臨床的に健康であり，かつ既知の病原微生物に感染していない場合であっても，サル類自身には特段の病原性を発揮せずに自然感染している微生物が，種を越えて人に感染した際に強い病原性を呈する可能性は否定できない。また実験的処置による免疫抑制状態において，サル類に自然感染している非病原性微生物が活性化すると考えられることから，実験内容により予防的措置が必要である。またサル輸送にともなうストレスでも同様の可能性があることから，導入時の検疫措置は不可欠である。当センターでは，施設内サルの安全確保のため，海外からの輸入あるいは他の国内施設からの導入サル全頭に対して検疫を実施している。検疫は，それら対象動物がどのような病原体に感染しているか不明であるが故に，少なくともBSL2病原体に対応が可能な動物施設で行うことが

必要であろう。

2）サルにおけるバイオハザード

①研究目的のためサル類に感染させた病原微生物が他のサル個体に施設内感染する可能性は常に考慮しなければならない。特にエアロゾル若しくは空気伝播しうる病原微生物（例：結核菌，麻疹ウイルス）では，こうした水平感染を予防するための措置が必要となる。

②サル類が自然感染している微生物が，他の個体に感染した際に病原性を呈する場合。例えばマカク属サルに感染が見られるサル水痘ウイルス（SVV）やタイプDサルレトロウイルス（SRV-D）は感染性，病原性共に強く，時としてサルコロニーに甚大な被害を与えることが知られている。またリスザルを自然宿主としているヘルペスウイルスサイミリ（HVS）はリスザル自体には病原性を有さないが，マーモセットやタマリンといった他の新世界ザルへの感染により重篤なリンパ性白血病を呈することから厳重な注意が必要である。

③人自身が感染している病原体がサル類に伝播するといったケースについても想定が必要である。結核や麻疹，風疹，インフルエンザなどに病原体取扱者が罹患している場合，動物施設内への入室を禁止，制限しなければならない。

バイオセーフティ管理のための基本とその概要

サル類を用いた病原性微生物の感染実験を行うための実験施設を安全に管理運営するに当たっては，ひとたびバイオハザード事故が起こればその被害は計り知れないものになる恐れがあることを念慮し，日常よりバイオハザードを防止するための安全対策が充分なされなければならない。バイオセーフティ対策としては，米国CDC/NIHが推奨するバイオセーフティレベルに応じた動物実験室基準を参考にすることが一般的である（表1）。基本的には，ハードウエアとソフトウエアにより安全確保する。

1）ハードウエア概要

第一にハードウエア，すなわち実験施設および病原体の安全操作に必要な設備による病原体の拡散を物理的に封じ込めることがバイオセーフティの前提であり最も重要である。これらは建築構造体および空調設備，安全キャビネット，サル用アイソレータ，オートクレーブ等機器類の正確な動作に依存するため，定期的メンテナンスによる保守管理はもちろんのこと，老朽化を前提とした計画的な整備計画が事故防止に不可欠である。またBSL3病原体を取扱う実験室では自家発電装置を設け，停電時にも設備機器機能が維持されるように備えておくことが必要である。これは災害発生時における病原体取扱者の安全確保に特に重要である。実際，2005年米国南部を襲ったハリケーン（カトリーナ）によりツーレン国立霊長類研究センターも甚大な被害を被ったが，充分な燃料備蓄を保有した自家発電装置により実験用サル類への被害を食い止めることができている。

2）ソフトウエア概要

前述のハードウエアを充分に機能させ，安全な病原体取扱を行うためには，バイオセーフティのための様々なルールが病原体取扱者によって遵守されなければならない。また必要に応じて病原体取扱者間による情報交換・問題提起，改善の場を設けることが望ましい。

（1）病原体取扱に関する各種規則の制定

現在我が国では，病原体取扱に関する法規制はなく（今年度改正された感染症法はバイオテロ対策が目的であり，病原体のバイオセーフティ管理といった面は必ずしも考慮されていない），そのため各研究機関等ごとに自主的な規制を設けている。多くの場合は国立感染症研究所の病原体等安全管理規程を基に，各研究機関や施設の状況を加味して策定されている。特に施設管理責任者や各病原体取扱におけるバイオセーフティ管理者を置くなどの安全管理態勢を確立し，責任の所在を明確化することが重要である。また具体的な病原体取扱方法や実験室への入退室，防護装備の着脱滅菌法，機器操作手順および緊急時の対応法などについてはそれぞれ安全操作マニュアルや危機対応マニュアルの作成が必要である。なおバイオハザードのリスクが高いABSL3施設では，外部委員を含む安全監視委員会を設け施設運営管理に関する定期的な審査・査察を実施することにより，バイオセーフティの判断に客観性を持たせることが望ましい。ちなみに当センターのABSL3施設では，外部委員を含む安全監視委員会による年1回の定期的査察を実施している。

（2）バイオセーフティに関する教育（再教育）の実施

病原体取扱者は，上記の各種規則のみならず，取扱う病

表1　微生物実験室のバイオセーフティ（CDC/NIH 監修，4th edition，1999 年発行）

動物実験施設のバイオセーフティレベル2（animal biosafety level 2：ABSL-2）基準
・動物用施設の管理者は，すべての操作および動物飼育舎への立入りの方針，手順およびプロトコルを確立しなければならない。
・職員用の適切な医療監視プログラムを設けなければならない。
・安全操作マニュアルを作成し，導入しなければならない。
・バイオハザード標示を扉および他の適切な場所に標示し，使用している感染性病原体を明示すること。
・施設は，掃除および維持管理が容易に行えるように設計しなければならない。
・扉は内側に開き，自動的に閉まる構造でなければならない。
・暖房，換気および照明は十分でなければならない。
・機械換気を行う場合，空気流は内側に向かっていなければならない。排気は屋外に排出し，建物のどの部分にも再循環しないこと。
・許可された者以外の立入りを制限しなければならない。
・実験用途以外の動物を入れないこと。
・節足動物およびげっ歯類防除対策を設けること。
・窓がある場合は，頑丈で耐破損性であり，開閉可能ならば節足動物を防ぐ網戸をはめなければならない。
・作業面の使用後は，効果的な消毒剤で汚染除去しなければならない。
・エアゾールの発生を伴う可能性のある作業には，HEPA フィルターを通して排気する安全キャビネット（クラスⅠまたはⅡ），または隔離飼育ケージを設けなければならない。
・現場または近くにオートクレーブを用意しなければならない。
・動物用床敷きの材料は，エアゾールおよび粉塵の発生を最小限に抑えるような方法で取り除かなければならない。
・すべての廃材および床敷きは，廃棄する前に汚染除去しなければならない。
・鋭利な機器の使用は，可能な限り禁止すること。鋭利物は必ず，穴の開かない蓋付きの容器に回収し，感染性のものとして扱うこと。
・オートクレーブまたは焼却する材料は，閉めた容器で安全に輸送しなければならない。
・動物ケージは，使用後汚染除去しなければならない。
・動物の死体は，焼却しなければならない。
・施設内では防護衣および装置を着用し，退出の際に脱がなければならない。適切な手袋を用意し，着用すること。
・手洗い設備を設けなければならない。職員は，動物用施設を退出する前に手を洗わなければならない。
・すべての外傷は，どんなに軽微なものでも報告し記録しなければならない。
・施設内では飲食および化粧を禁じなければならない。
・すべての作業者は，適切な教育訓練を受けなければならない。

動物実験施設のバイオセーフティレベル3（animal biosafety level 3：ABSL-3）基準
・ABSL-2 のすべての要件を満たさなければならない。
・立入りを厳密に管理しなければならない。
・扉を2つ備える部屋によって控え室を形成し，施設を他の実験室および動物舎から区画しなければならない。
・更衣室に手洗い設備およびシャワーを設けなければならない。
・全室に確実に連続した空気を流すため，機械換気を行わなければならない。排気は再循環させず，大気に放出する前に HEPA フィルターを通さなければならない。換気システムは，不測の逆流が生じず，動物舎のどの部分も昇圧しないように設計しなければならない。
・動物舎内の生物危害が収容されている場所に好都合の位置に，オートクレーブを用意しなければならない。感染性廃棄物は，施設の他の区域に移動される前にオートクレーブすること。
・BSL3 病原体に感染させた動物は，アイソレーター内のケージ，またはケージ後部に換気の排気装置を配置した部屋で飼育しなければならない。
・床敷きは，可能な限り粉塵がないようにすること。
・施設内では，実験室用防護衣を着用しなければならない。この防護衣は実験室外に退出する前に汚染除去しなければならない。
・窓は閉めて密閉し，耐破損性でなければならない。
・必要に応じて，職員に予防接種を行うこと。

原体ごとの性状（BSL 分類，感染様式，病原性など）や滅菌方法などの基本知識を把握していることが不可欠である。またサル類を用いる動物実験を実施する場合には，サル類ごとの特性に基づく取扱い方法にも習熟していなければならない。このため，定期的なバイオセーフティ講習会を実施し病原体取扱者の受講（必要に応じてペーパーテストや実習を行う）を義務づけるようにする。なお新規病原体を用いようとする研究者は，施設管理者や動物技術者等への病原体に関する情報（不活化方法，リスク評価，事故時の対応法など）を公開し，充分な安全対策を図るようにする。

（3）特別定期健康診断の実施

前述の実験用霊長類を用いる感染症モデル研究実施におけるバイオハザードの可能性を考慮し，病原体取扱者に対して年１～２回程度の特別定期健康診断受診を義務化する。特に結核予防のため，胸部Ｘ線撮像による診断が不可欠である。取り扱う病原体により，医師による診察や抗体価測定検査を実施し，また必要に応じてワクチンの接種を勧告し，職員等も職務上必要と考えられる場合はワクチンの接種を要求できるようにする。さらに，健康診断の結果に基づき，健康管理上必要と認められる事項については病原体取扱者ごとに記録を作成し保存することが大切である。

なお病原体取扱に際しては，万が一の病原体への暴露事故が生じた場合にその病原体への感染有無を評価する目的で血清の採取・保存を実施する。血清の採取・保存は予め承諾を得た上で行い，その使用に当たっては，個人（退職者を含む）の健康障害の発生またはそのおそれのある場合に限り，バイオセーフティ委員会の承認の下で行うこととする。なお，これら健康診断，血清保存に関する病原体取扱者の個人情報については，充分かつ適切な保護がなされなければならない。

（4）運営会議の実施

病原体取扱者（特に施設管理者，飼育管理技術者，獣医師など施設運営実務者）間における情報交換・問題提起，改善の場として運営会議を定期的に設けることが望ましい。特にサル類を用いる病原体感染実験では，既に述べたようにバイオセーフティ以外にも様々なコンプライアンスが求められることから，実務者個人の当事者意識の向上が安全かつ健全な施設運営のために非常に重要である。

終わりに

本項では，バイオセーフティの観点から，医学実験用霊長類を用いた病原体感染実験施設の管理運営におけるコンプライアンスについて当センターにおける例を挙げながら概説した。特にバイオセーフティ管理は自主規制であることからそのルール徹底が難しく，また特殊施設であるがための維持管理経費も莫大なものとなる。しかしながら狂牛病やSARSにおける経緯からわかるように，経済立国である我が国にとって新興再興感染症の予防治療対策は必須のものであり，そのトランスレーショナルリサーチにおいて医学実験用霊長類を用いた病原体感染実験施設は今後さらにその重要性を増すものと思われる。

稿を終えるに当たり，当施設の管理運営にご協力いただいた疾患制御研究室および社団法人予防衛生協会の職員各位に深謝したい。

Laboratory Animals

Vet Pathol 45:67–72 (2008)

BRIEF COMMUNICATIONS and CASE REPORTS

Transthyretin Amyloidosis and Two Other Aging-Related Amyloidoses in an Aged Vervet Monkey

S. NAKAMURA, S. OKABAYASHI, N. AGEYAMA, H. KOIE, T. SANKAI, F. ONO, K. FUJIMOTO, AND K. TERAO

The Corporation for Production and Research of Laboratory Primates, Tsukuba, Ibaraki, Japan (SN, SO, FO, KF); Tsukuba Primate Research Center, National Institute of Biomedical Innovation, Tsukuba, Ibaraki, Japan (NA, TS, KT); and the Department of Veterinary Medicine, College of Bioscience, Nihon University, Fujisawa, Kanagawa, Japan (HK)

Abstract. An aged male vervet monkey showed severe cardiac arrhythmia for more than 3 years. A multifocal amyloid consisting of transthyretin was deposited in all areas of the heart wall, especially in the extracellular stroma among muscle fibers and external tunica of arterioles. Moreover, the amyloid was deposited in the stroma and arterioles of other systemic organs except the liver and spleen. These characteristics are consistent with senile systemic amyloidosis in humans. A second amyloid consisting of amyloid β protein was in senile plaques and cerebral amyloid angiopathy in the cerebral cortex. A third amyloid consisting of islet amyloid polypeptide was deposited in islets of the pancreas. Apolipoprotein E and amyloid P component colocalized with the 3 amyloids. Thus, 3 different aging-related amyloids were found in an aged vervet monkey. In particular, to our knowledge, this is the first report on spontaneous transthyretin amyloidosis in animals.

Key words: Amyloidosis; amyloid β protein; IAPP; transthyretin.

Amyloid is a degenerative protein that exhibits common biochemical and morphologic characteristics, such as 1) birefringence under polarizing microscope, 2) abundant β pleated–sheets in the secondary structure of the proteins, and 3) nonbranching and nonparallel straight fibrils (8–10 nm in diameter) under electron microscope.[13] However, each amyloid consists of different precursor proteins.[13] Furthermore, amyloidosis may develop secondary to various conditions, such as inflammation, aging, and certain neoplasms. Transthyretin (TTR), amyloid β protein (Aβ), and islet amyloid polypeptide (IAPP) amyloidoses are well known as major aging-related amyloidoses.[15] Among these amyloids, senile systemic amyloidosis (SSA), which is characterized by the deposition of amyloid fibrils containing TTR, is well known in aged humans but not in animals. In SSA, first small amyloid deposits, mainly in the heart, occur without obvious symptoms. However, in some case, massive amyloid deposits result in heart failure, eventually leading to death.[15]

In nonhuman primates, limited literature on amyloidosis is available. However, cerebral Aβ and islet amylin amyloidoses have been investigated in nonhuman primates as models for Alzheimer's disease and diabetes mellitus, respectively.[7,10] In the vervet monkey, there has only been one report on cerebral Aβ deposition preventable by Aβ vaccination,[4] whereas no study has been conducted for other types of amyloidoses.

A male vervet monkey (*Cercopithecus aethiops*), assumed to be 29 years old, showed severe cardiac arrhythmia for more than 3 years and bradycardia at the later stage of the 3 years, which were detected by 4-leads electrocardiography. Premature ventricular contractions (PVCs) were monitored by 24-hour Holter electrocardiography. The frequency of PVCs gradually became severe (3,000 PVCs per day) during the 3 years. Moreover, dilatation of the right ventricle was detected by ultrasound and X-ray examinations. However, for the left ventricle, no obvious disorders, such as reduced left ventricular ejection fractions, were observed by echocardiography. Symptoms associated with Alzheimer's disease and diabetes mellitus were not observed in the present case. Finally, the monkey was euthanized because of poor prognosis due to severe depression and anorexia.

At necropsy, collected tissues were fixed in 10% buffered formalin, embedded in paraffin, and sectioned at 4 μm. The deparaffinized sections were stained with hematoxylin and eosin. Some sections were stained with Congo red and direct fast scarlet (DFS; Muto, Tokyo,

Fig. 1. Heart; Vervet monkey. Heart revealed slight dilatation with various sized pale white spots on the surface. Bar = 1 cm.

Japan) with or without potassium permanganate (PPM). Positive reactions for Congo red and DFS were confirmed by apple green birefringence under polarizing microscope. Furthermore, some deparaffinized sections were immunostained using rabbit polyclonal antibodies against Aβ 1–42 (Aβ42; Chemicon, Temecula, CA; 1:100), amyloid P component (AP; DAKO, Glostrup, Denmark; 1:300), apolipoprotein E (apoE; DAKO; 1:1000), calcitonin (IBL, Takasaki, Japan; 1:400), kappa light chains (κAL; DAKO; 1:20000), lambda light chains (λAL; DAKO; 1:40000), and TTR (DAKO; 1:100) and using mouse monoclonal antibodies against amyloid A (AA; Novocastra, Newcastle, UK; 1:100) and IAPP (Serotec, Raleigh, NC; 1:100). Sections immunostained for Aβ42 were pretreated with 99% formic acid for 10 minutes. The remaining immunostains used pretreatment with citrate buffer (pH 6.0, 121°C, 10 min). These sections were further reacted with horseradish peroxidase-conjugated secondary mouse and rabbit immunoglobulins (EnVision+ System, DAKO) and then visualized with 3,3′-diaminobenzidine tetrahydrochloride (DAB).

At necropsy, the heart revealed slight dilatation of both ventricles with thinning of the right ventricular free wall. The surface of the heart was reddish brown with pale white spots (Fig. 1). The brain and pancreas showed slight atrophy.

Myocardium and stroma were multifocally replaced by hyaline material deposits, mainly in the free wall of the ventricles (Fig. 2). Hyaline deposits were observed regardless of the area in the heart, such as subendocardium or subepicardium and right or left wall. They showed uniform pale pink staining with hematoxylin and eosin in the extracellular stroma among the heart muscle fibers (Fig. 3). These hyaline deposits were positive for DFS and Congo red (Fig. 4, Table 1), and their reactions were resistant to PPM (data not shown). DFS and Congo red stained the hyaline deposits; however, DFS showed less nonspecific background than did Congo red. Apple green birefringence corresponding to their hyaline deposits was observed by both DFS and Congo red under polarizing microscope (data not shown). The intensity of birefringence was stronger with Congo red than with DFS (data not shown). Moreover, in the heart, DFS- and Congo red–positive deposits were observed in the external tunica of some arterioles. These cardiac amyloids were immunohistochemically positive for antibodies against TTR, apoE, and AP (Fig. 5, Table 1). The intensity of TTR immunoreactivity was most significant. Moreover, immunoreactivity of TTR as well as of apoE was greater than that of AP. Heart muscle fibers adjoining the amyloid lesions showed necrotic or atrophic changes (Fig. 3).

Hyaline deposits were found mainly in the stromal connective tissues (fibrous and adipose tissues) and external tunic of the blood vessels. Moreover, faint deposits were observed in the peripheral nerves of the thyroid gland, tonsil, salivary glands, thymus, prostate gland, lymph nodes, and skeletal muscles (Table 1). As for mucosal organs, the deposits were found in lamina propria of the tongue, trachea, esophagus, stomach, intestines, and urinary bladder; submucosal layers of the stomach and intestines; muscular layer of the intestines and urinary bladder; and serosa of the trachea and esophagus (Table 1). Furthermore, hyaline deposits in the lungs were found in the alveolar walls, bronchial wall, and external tunica of arterioles (Table 1). In the kidneys, the deposits were detected in the renal pelvis and external tunica of the arcuate arteries (Table 1). In these organs, severe deposits were found in the thyroid gland, tongue, esophagus, and stomach; moderate deposits in the tonsil, thymus, lungs, intestines, and skeletal muscles; and weak deposits in the salivary glands, trachea, kidneys, urinary bladder, and lymph nodes. These deposits were positive for DFS and Congo red (Table 1) but resistant to PPM and revealed apple green birefringence under polarizing microscope (data not shown). These were immunohistochemically positive for antibodies against TTR, apoE, and AP (Table 1). The intensity of immunoreactivity was stronger for TTR and apoE than for AP. Furthermore, TTR-positive but DFS- and Congo red–negative lesions were detected in the external tunica of blood vessels of the testes. Reactivity for DFS and Congo red and immunoreactivity of TTR, apoE, and AP were not detected in the liver, spleen, pituitary, and adrenal gland (Table 1). Thus, based on histochemical and immunohistochemical characteristics of cardiac and other amyloids, systemic amyloidosis characterized by the deposition of amyloid fibrils containing TTR was confirmed.

The second type of hyaline deposit, such as neuritic senile plaques (SPs), was observed in the cerebral cortices. DFS and Congo red detected not only some neuritic SPs but also deposits consistent with cerebral amyloid angiopathy (CAA) (Table 1), as found previously in vervet and cynomolgus monkeys.[4,5] This type of amyloid was resistant to PPM and revealed apple green birefringence under polarizing microscope (data

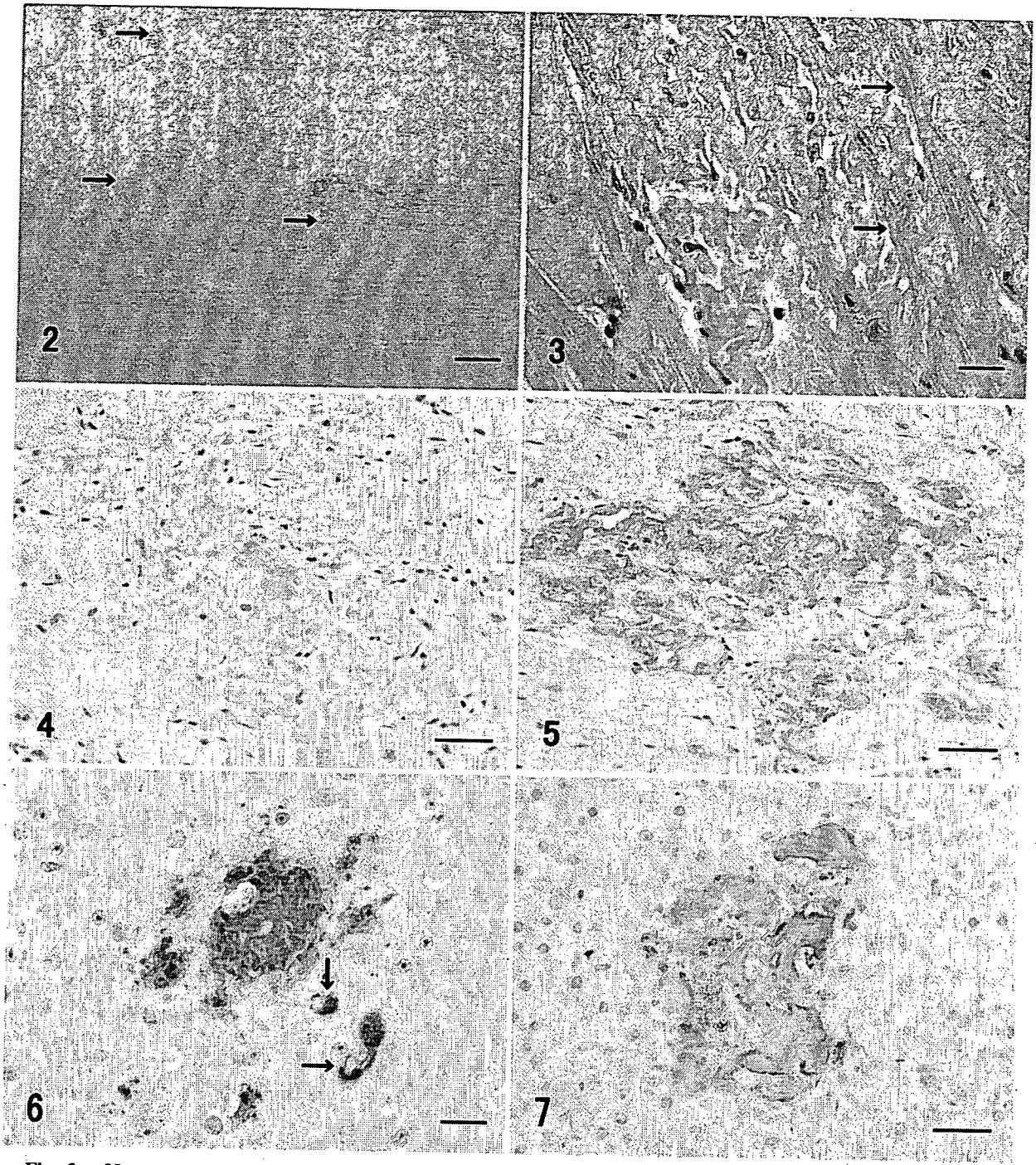

Fig. 2. Heart; vervet monkey. Hyaline deposits (arrows) were multifocally found in the heart wall. HE. Bar = 200 μm.
Fig. 3. Heart; vervet monkey. Hyaline materials showed uniform pale pink staining, and the surrounding muscle fibers revealed atrophic and necrotic changes (arrows). HE. Bar = 20 μm.
Fig. 4. Heart; vervet monkey. Hyaline materials were positive for direct fast scarlet (DFS). DFS. Bar = 50 μm.
Fig. 5. Heart; vervet monkey. Amyloid deposits were immunohistochemically positive for antibodies against transthyretin. Immunoperoxidase method, hematoxylin counterstain. Bar = 50 μm.
Fig. 6. Cerebrum; vervet monkey. Cerebral amyloid deposits, such as neuritic senile plaques and capillary-cerebral amyloid angiopathy (arrows), were immunohistochemically positive for antibodies against amyloid β protein. Immunoperoxidase method, hematoxylin counterstain. Bar = 20 μm.
Fig. 7. Pancreas; vervet monkey. Islet amyloid deposits were immunohistochemically positive for antibodies against islet amyloid polypeptide (IAPP). Immunoperoxidase method, hematoxylin counterstain. Bar = 20 μm.

Table 1. Histochemical and immunohistochemical features of amyloid depositions in various organs and tissues of an aged vervet monkey.

Organ or Tissue	DFS*	Congo Red	TTR	Aβ	IAPP	apoE	AP	Notes
Brain	++	+	−	+++	−	++	+	Senile plaques and amyloid angiopathy
Pituitary	−	−	−	−	−	−	−	
Thyroid	+++	++	+++	−	−	+++	+++	Parafollicular areas
Parathyroid	−	−	−	−	−	−	−	
Tongue	+++	+++	+++	−	−	+++	+++	Tunica propria, stroma, and blood vessels
Tonsil	++	+	++	−	−	+++	++	Stroma and adjoining connective tissues
Salivary	+	+	+	−	−	+	+	Stroma, blood vessels, and adjoining connective tissues
Trachea	+	+	++	−	−	+	+	Tunica propria and serosa
Esophagus	+++	+++	+++	−	−	+++	+++	Tunica propria, muscle layer, and serosa
Heart	+++	+++	+++	−	−	+++	+++	Myocardium and blood vessels
Thymus	++	++	+++	−	−	+++	++	Stroma and adjoining connective tissues
Lungs	++	++	+++	−	−	+++	+++	Alveolar and bronchus walls and blood vessels
Stomach	+++	+++	+++	−	−	+++	++	Tunica propria, submucosal and muscle layer, and blood vessels
Intestines	++	++	+++	−	−	+++	++	Tunica propria, muscle layer, and blood vessels
Pancreas	++	++	−	−	+++	+++	++	Islets
Liver	−	−	−	−	−	−	−	
Gall bladder	−	−	−	−	−	−	−	
Spleen	−	−	−	−	−	−	−	
Kidneys	+	+	+	−	−	+	+	Renal pelvis and arcuate arteries
Adrenal	−	−	−	−	−	−	−	
Testes	−	−	+	−	−	−	−	Blood vessels
Prostate	+++	+++	+++	−	−	+++	+++	Stroma and blood vessels
Urinary bladder	+	+	+	−	−	+	+	Muscle layer and blood vessels
Lymph nodes	+	+	++	−	−	++	+	Stroma, blood vessels, and adjoining connective tissues
Skeletal muscle	++	++	++	−	−	++	+	Stroma and blood vessels
Sciatic nerve	−	−	−	−	−	−	−	
Bone	−	−	−	−	−	−	−	
Bone marrow	−	−	−	−	−	−	−	
Skin	NT	NT	NT	NT	NT	NT	NT	

*DFS = direct fast scarlet; TTR = transthyretin; Aβ = amyloid β protein; IAPP = islet amyloid polypeptide; apoE = apolipoprotein E; AP = amyloid P component.

+++ = strong positive; ++ = moderate positive; + = weak positive; − = negative; NT = not tested.

not shown). Furthermore, SPs and CAA were immunohistochemically labeled using antibodies against Aβ42, apoE, and AP (Fig. 6, Table 1). The intensity of immunoreactivity was stronger with Aβ42 and apoE than with AP. Diffuse plaques, found previously in cynomolgus monkeys,[5] were not found in the present case. This amyloid derived from Aβ was not deposited in the other organs (Table 1).

The third type of hyaline deposit was found in the expanded stromal areas of islets of the pancreas. This was positive for Congo red and DFS and resistant to PPM (Table 1) and showed apple green birefringence under polarizing microscope (data not shown). This amyloid was immunohistochemically positive for antibodies against IAPP, apoE, and AP (Fig. 7, Table 1). The intensity of immunoreactivity was stronger with

IAPP and apoE than with AP. The islets, where abundant amyloid was deposited, had a reduced number of islet cells. This IAPP-derived amyloid was not detected from any other organ (Table 1).

Finally, all the 3 types of hyaline deposits were immunohistochemically negative for antibodies against AA, calcitonin, κAL, and λAL (Table 1).

Although there is no information about amino acid sequences of TTR, Aβ, and IAPP in vervet monkeys, the sequences in human are 93.1%, 100%, and 94.6% homology (BAC20609 and XP_001098180),[11] respectively, against those in macaque monkeys and vervet monkeys, who belong taxonomically to *Cercopithecus*. Antibodies to TTR and Aβ used in the present study have reacted with each amyloid lesion, that is, cardiac amyloid in SSA and SPs in AD, consisting of intact mature amyloid in human.[8,12] The immunoreactivities of humans were absolutely corresponding to that of this vervet monkey. According to these facts, we assumed that these antibodies recognized suitable TTR and Aβ amyloid lesions in vervet monkeys, as well as humans. On the other hand, as for IAPP, detail immunohistochemical information of an antibody to IAPP 7–17 residue used in this study has not been described, while similar antibodies to IAPP 8–17 residue reacted well with intact islet amyloid in humans and cats.[6] The immunoreactivity of an antibody to IAPP 8–17 was consistent with that of an antibody to IAPP 7–17. Those IAPP residues are conserved between various mammalian species, and IAPP 8–20 is known as the second major constituent of islet amyloid.[5] Therefore, we assumed that the antibody to IAPP used in this study reacted precisely with intact islet amyloid of this monkey species.

SSA is one of the common systemic amyloidoses in humans, occurring in 25% of people who are older than 80 years.[15] SSA has been previously called cardiac amyloidosis because it shows cardiac symptoms, such as heart failure and/or arrhythmia, due to severe amyloid deposition in the heart.[15] As for histopathologic characteristics of SSA in humans, the organ most severely affected by amyloid deposition is the heart, while deposition is also found in the other systemic organs. On the other hand, there are few amyloid deposits in the liver, spleen, and kidney, except the renal pelvis, which are frequent organs for other types of systemic amyloidoses, such as AA or AL amyloidosis.[15] These histopathologic features in humans are consistent with those in the vervet monkey. Furthermore, clinical symptoms, such as arrhythmia, and biochemical aspects of the amyloid precursor, such as TTR and not AA or AL, in humans, correspond to the characteristics in the vervet monkey.[14] Another manifestation of TTR amyloid deposition is familial or hereditary TTR amyloidosis, which is known as familial amyloid polyneuropathy (FAP).[15] FAP patients with a variant TTR reveal onset of cardiac symptoms and severe systemic TTR amyloidosis usually the third decade of life, with deposits especially prominent in the heart and peripheral nervous system.[13] Because there is no information for TTR amino acid sequence and its mutant in vervet monkeys, the hereditary aspect of TTR amyloidosis could not be considered in the present study. However, the clinical, histologic, and immunohistochemical features suggest that the monkey suffered from SSA and not FAP, because the monkey was very old (a 29-year-old monkey corresponds nearly to an 85-year-old human) and because amyloid was deposited exclusively in the heart rather than in the peripheral nerves.

Teng and colleagues[14] reported that transgenic mice overexpressing human wild-type *TTR* gene revealed predominant deposits of TTR-positive and DFS-negative materials in the heart and kidney. This type of deposit is consistent with the deposits in the testes of the vervet monkey in this study. Namely, the deposits in TTR transgenic mice and this vervet monkey may be considered immature materials before amyloid fibril formation.[14]

Cerebral amyloidosis consisting of Aβ is an aging-related amyloidosis, although it occurs earlier and is significantly developed in Alzheimer's disease.[6,8] SPs and CAA as histopathologic hallmarks in Alzheimer's disease also appear in aged nonhuman primates.[7] SPs in cynomolgus monkeys are morphologically classified into neuritic and diffuse plaques; the neuritic plaques are more frequently observed than the diffuse ones, whereas CAA is more frequently found in capillaries than in meningeal arterioles.[7] Findings of abundant neuritic plaques and predominant capillary CAA rather than meningeal CAA have been described previously, in the first study of SPs and CAA in a vervet monkey.[4] The characteristics of SPs and CAA in the present study are consistent with the previous studies of cynomolgus monkeys.[7]

Islet amyloidosis consisting of IAPP often appears as one of the aging-related changes in aged primates including humans,[3] while this amyloid deposition is accelerated in diabetes mellitus.[13] Because the vervet monkey did not have any history for diabetes, possibilities are considered that the islet amyloid deposition in this monkey likely occurred as an aging-related change and that degrading insulin secretion in the absence of fasting hyperglycemia was associated with an increase of IAPP aggregation and the onset of islet amyloidosis.[3] This type of amyloid deposition has been previously reported in various primate species, that is, humans and macaque monkeys.[10,13] Morphologic and immunohistochemical characteristics of islet amyloidosis in vervet monkey are consistent with those in other primate species.[10]

ApoE and AP are often colocalized with various types of amyloid precursors, such as Aβ, prion protein, AA, and IAPP[7,9,13] and accelerate in vitro fibril formation of the amyloids.[1] Although in vitro data on the correlation between apoE and TTR have not been confirmed previously, the colocalization of apoE in the TTR amyloid portion suggests that TTR amyloid deposition might be accelerated by apoE and AP, as well as other types of amyloids.[13] In summery, 3 different aging-related amyloidoses were found in an

aged vervet monkey. TTR amyloidosis has only been reported in SAMP mice,[2] while this is the first spontaneous case report on TTR amyloidosis in mammalian species, other than humans and experimental animals with a special genetic background.

Acknowledgement

The authors thank Ms. Chieko Ohno for her technical help.

References

1 Hass S, Fresser F, Kochl S, Beyreuther K, Utermann G, Baier G: Physical interaction of ApoE with amyloid precursor protein independent of the amyloid Aβ region in vitro. J Biol Chem **273:**13892–13897, 1998

2 Higuchi K, Naiki H, Kitagawa K, Hosokawa M, Takeda T: Mouse senile amyloidosis: ASSAM amyloidosis in mice presents universally as a systemic age-associated amyloidosis. Virchows Arch B Cell Pathol Incl Mol Pathol **60:**231–238, 1991

3 Hull RL, Westermark GT, Westermark P, Kahn SE: Islet amyloid: a critical entity in the pathogenesis of type 2 diabetes. J Clin Endocrinol Metab **89:**3629–3643, 2004

4 Lemere CA, Beierschmitt A, Iglesias M, Spooner ET, Bloom JK, Leverone JF, Zheng JB, Seabrook TJ, Louard D, Li D, Selkoe DJ, Palmour RM, Ervin FR: Alzheimer's disease Aβ vaccine reduces central nervous system Aβ levels in a non-human primate, the Caribbean vervet. Am J Pathol **165:**283–297, 2004

5 Mazor Y, Gilead S, Benhar I, Gazit E: Identification and characterization of a novel molecular-recognition and self-assembly domain within the islet amyloid polypeptide. J Mol Biol **322:**1013–1024, 2002

6 Ma Z, Westermark GT, Johnson KH, O'Brien TD, Westermark P: Quantitative immunohistochemical analysis of islet amyloid polypeptide (IAPP) in normal, impaired glucose tolerant, and diabetic cats. Amyloid **5:**255–256, 1998

7 Nakamura S, Kiatipattanasakul W, Nakayama H, Ono F, Sakakibara I, Yoshikawa Y, Goto N, Doi K: Immunohistochemical characteristics of the constituents of senile plaques and amyloid angiopathy in aged cynomolgus monkeys. J Med Primatol **25:**294–300, 1996

8 Nagele RG, D'Andrea MR, Anderson WJ, Wang HY: Intracellular accumulation of β-amyloid$_{1-42}$ in neurons is facilitated by the alpha 7 nicotinic acetylcholine receptor in Alzheimer's disease. Neuroscience **110:**199–211, 2002

9 Namba Y, Tomonaga M, Kawasaki H, Otomo E, Ikeda K: Apolipoprotein E immunoreactivity in cerebral amyloid deposits and neurofibrillary tangles in Alzheimer's disease and kuru plaque amyloid in Creutzfeldt-Jakob disease. Brain Res **541:**163–166, 1991

10 O'Brien TD, Wagner JD, Litwak KN, Carlson CS, Cefalu WT, Jordan K, Johnson KH, Butler PC: Islet amyloid and islet amyloid polypeptide in cynomolgus macaques (*Macaca fascicularis*): an animal model of human non-insulin-dependent diabetes mellitus. Vet Pathol **33:**479–485, 1996

11 Podlisny MB, Tolan DR, Selkoe DJ: Homology of the amyloid β protein precursor in monkey and human supports a primate model for β amyloidosis in Alzheimer's disease. Am J Pathol **138:**1423–1435, 1991

12 Sawabe M, Hamamatsu A, Ito T, Arai T, Ishikawa K, Chida K, Izumiyama N, Honma N, Takubo K, Nakazato M: Early pathogenesis of cardiac amyloid deposition in senile systemic amyloidosis: close relationship between amyloid deposits and the basement membranes of myocardial cells. Virchows Arch **442:**252–257, 2003

13 Sipe JP: 2005 Amyloid Proteins, 1st ed., pp. 3–27, pp. 180–181, pp. 385–406, pp. 732–742. WILEY-VCH, Weinheim, Germany, 2005

14 Teng MH, Yin JY, Vidal R, Ghiso J, Kumar A, Rabenou R, Shah A, Jacobson DR, Tagoe C, Gallo G, Buxbaum J: Amyloid and nonfibrillar deposits in mice transgenic for wild-type human transthyretin: a possible model for senile systemic amyloidosis. Lab Invest **81:**385–396, 2001

15 Westermark P, Bergstrom J, Solomon A, Murphy C, Sletten K: Transthyretin-derived senile systemic amyloidosis: clinicopathologic and structural considerations. Amyloid **10**(Suppl 1): 48–54, 2003

Request reprints from Shinichiro Nakamura, Research Center for Animal Medical Science, Shiga University of Medical Science, Seta-Tsukinowa-Cho, Ohtsu, Shiga 520-2192 (Japan). E-mail: snakamur@belle.shiga-med.ac.jp.

Reproductive Medicine and Biology 2007; 6: 203–210 doi: 10.1111/j.1447-0578.2007.00186.x

Original Article

Collection and culture of primordial germ cells from cynomolgus monkeys (*Macaca fascicularis*)

HIRONORI OKADA,[1] MASANORI HATORI,[1,2] NOBUHIRO SHIMOZAWA,[1] HIDEAKI TSUCHIYA,[3] TAKASHI KUWANA[4] and TADASHI SANKAI[1]*

[1]*Tsukuba Primate Research Center, National Institute of Biomedical Innovation,* [2]*Graduate School of Comprehensive Human Sciences, University of Tsukuba,* [4]*Laboratory of Intellectual Fundamentals for Environmental Studies, National Institute for Environmental Studies, Ibaraki, and* [3]*Research Center for Animal Life Science, Shiga University of Medical Science, Shiga, Japan*

Aim: To clarify the location of primordial germ cells (PGC) in an embryo of target-age and to examine the culture environment of the PCG.

Methods: The days of ovulation and fertilization were estimated by measuring the serum concentration of estrogen. Pregnancy was confirmed by measurement of the serum concentration of the beta subunit of macaque chorionic gonadotropin and by ultrasonography. We also examined the location of PGC in the embryo at the time of retrieval.

Results: Results showed that PGC in an embryo were in the hindguts at day 30 postfertilization, arrived at the genital ridges via mesenteries at approximately day 33 postfertilization, and colonized the gonads by day 36 postfertilization.

Conclusions: In conclusion, embryos collected on day 33 postfertilization are more suitable for obtaining PGC from cynomolgus monkeys. The PGC collected from cynomolgus monkey fetuses were cultured under conditions for the derivation and culture of human embryonic germ cells; enzymatically dispersed single cells were cultured on a SIM thioguanine-resistant ouabain-resistant cells (STO) feeder layer with recombinant human leukemia inhibitory factor, recombinant human basic fibroblast growth factor and forskolin. The cells from genital ridges and mesenteries at day 33 postfertilization had alkaline phosphatase (ALP) activity *in vitro* for a maximum of 13 days. In contrast, ALP activity had been held for 2 months under the same culture condition when the cells were derived from the gonads at day 66 postfertilization. Derivation of an embryonic germ cell from a cynomolgus monkey was not achieved from these cultures. (Reprod Med Biol 2007; 6: 203–210)

Key words: cynomolgus monkey, embryo, pregnancy diagnosis, primordial germ cell.

INTRODUCTION

RESEARCH INTO PLURIPOTENT stem cells, such as embryonic stem (ES) cells, has been active because of its application to regenerative medicine. In basic research, mouse and non-human primates are often used. Cynomolgus monkeys are, therefore, a crucial animal model for evaluating the safety of regenerative medicine.[1] Because embryonic germ (EG) cells derived from human primordial germ cells (PGC) have a similar pluripotency to ES cells, except for the inability to form teratoma, such EG cells will become a source of pluripotent stem cells for regenerative medicine.[2,3] However, details of the behavior of PGC are unclear in most mammals, including cynomolgus monkeys. As a first step in the development of an evaluation system for the differentiation potential of EG cells using cynomolgus monkeys and for biological basic research, we attempted to obtain an embryo of a target age, and to examine the location of PGC in the embryo at the time of retrieval. In addition, we examined the culture environment of PGC from a cynomolgus monkey.

Correspondence: Dr Tadashi Sankai, Tsukuba Primate Research Center, National Institute of Biomedical Innovation, Hachimandai 1-1, Tsukuba, Ibaraki 305-0843, Japan. Email: sankai@nibio.go.jp
Received 16 April 2007; accepted 26 June 2007.

MATERIALS AND METHODS

Animals

THIS STUDY USED sexually mature male and female cynomolgus monkeys that had been bred

and maintained at the Tsukuba Primate Research Center, National Institute of Biomedical Innovation, Ibaraki, Japan.[4] The monkeys were housed in a room maintained at 25 ± 2°C with a relative humidity of 60 ± 5% and a 14 h/10 h light/dark cycle (lights on from 0500 to 1900 hours). The monkeys were fed apples (100 g each) every morning and commercial monkey diet every afternoon (70 g each; Type AS, Oriental Yeast; calcium content was approximately 1.5%).

Protocols for all experiments involving animals in this study were in compliance with the guidelines set by the National Institutes of Biomedical Innovation for the care, use and biological hazard countermeasures of laboratory animals.

Pairing and pregnancy diagnosis during the early pregnancy period

Female cynomolgus monkeys were paired in a cage with a sexually mature male from day 10 of their menstrual cycle to the day of ovulation. Ovulation in the menstrual cycle of the females was estimated by measuring the serum concentration of estrogen using a commercially available enzyme immunoassay (EIA) kit for human hormones (IMx system; Dainabot, Tokyo, Japan). Blood samples were taken on the morning of day 9 of the menstrual cycle and during the pairing period, and sera separated by centrifuge were frozen until measurements were taken. The day of ovulation was estimated to be the day that the estrogen concentration decreased. Pregnancy of a female was confirmed both by an increase in the serum concentration of the beta subunit of macaque chorionic gonadotropin (β-mCG) and by the presence of a gestational sac and heartbeat of an embryo. The serum concentration of β-mCG was measured using the IMx system with the kit for measurement of the beta subunit of human chorionic gonadotropin (β-hCG), according to manufacturer's instructions for measuring the serum concentration of β-hCG. Blood samples were taken on the morning of 1 day during week 4 postovulation. The presence of a gestational sac and heartbeat was confirmed using ultrasonography during week 5 postovulation.

Embryo collection

Uteruses with oviducts and ovaries were extracted from pregnant cynomolgus monkeys that were killed by sodium pentobarbital overdose on day 30, 33, 36 or 66 postovulation. Embryos were then extracted from the uteruses. Dissection was carried out using a dissection microscope. Gonads were extracted from the embryos at day 36 and 66 postovulation, genital ridges and mesenteries at day 33 postovulation, and urogenital ridges (with mesenteries) and hindgut (near the base of the allantoises) at day 30 postovulation.

Histochemistry and alkaline phosphatase staining for primordial germ cell identification

The gonads from one side were fixed with Rossman's fixture overnight at 4°C, dehydrated in the general manner, and mounted in paraffin. Serial sections were cut at 10 μm and mounted on glass slides. Specimens were then deparaffinized with xylene and hydrated by washing with the following series: 100% ethanol, 100% ethanol, ethanol containing 0.5% celoidine 100% ethanol, 70% ethanol, tap water, and finally distilled water. For staining with periodic acid Schiff (PAS) stain, the slides were immersed in 0.5% periodate for 10 min, washed with distilled water followed by tap water, immersed in Schiff's reagent for 20 min, immersed in sodium bisulfite solution for 5 min, and washed in tap water and finally in distilled water. Optionally, the slides were immersed in hematoxylin staining solution for 30 s and then rashly washed in tap water and finally in distilled water. After dehydration using an ethanol series with 70%, 80%, 90%, 95% and 100% ethanol solutions, the slides were dipped in xylene and covered by glass coverslips with Permount (Fisher Scientific Japan, Yokohama, Japan). Alkaline phosphatase activity of the gonads from the other side was measured using an alkaline phosphatase substrate kit I (VECTOR Red Alkaline Phosphatase Substrate Kit I; Vector Laboratories, Burlingame, USA) according to the manufacturer's instructions after 32 h culture with α-modified minimum essential medium supplemented with 10% fetal bovine serum (FBS) in 5% CO_2 at 37°C.

Cell culture of cynomolgus monkey embryos

Genital ridges and mesenteries were cut from cynomolgus monkey embryos on day 33 postovulation. Urogenital ridges, mesenteries and hindguts were mechanically minced into cell clumps. These cell clumps were briefly exposed to phosphate buffered saline (PBS) containing 0.1% Trypsin and 0.02% ethylen diamin tetra acetat (Trypsin-EDTA) to slightly disperse the cells. After washing with PBS, the cells were cultured with Dulbecco's Modified Eagle's Medium (DMEM) supplemented with 10% FBS, 1000 U/mL recombinant human leukemia inhibitory factor (rhLIF) and 1 ng/mL recombinant

human basic fibroblast growth factor (rhbFGF) in 5% CO_2 at 37°C. When the cells growing around the cell clumps become confluent, colonies from the cell clumps were removed after brief exposure to Trypsin-EDTA, and finally placed on a feeder layer of cynomolgus monkey embryonic fibroblasts that were collected from the respective embryos and that were mitotically inactivated by mitomycin C.

In another experiment, genital ridges collected on day 33 postovulation and gonads collected on day 66 postovulation were dispersed into single cells using Trypsin-EDTA and cultured on a mouse SIM thioguanine-resistant ouabain-resistant cells (STO) fibroblast feeder layer that had previously been mitotically inactivated by mitomycin C. The cells were then cultured in DMEM supplemented with 10% FBS, 1000 U/mL rhLIF, 1 ng/mL rhbFGF and 10 μmol/L forskolin. These cells were enzymatically disaggregated to single cells every 5–9 days, and were subcultured on a fresh STO feeder layer in fresh medium.

Cell staining for the detection of primordial germ cells after culture

Cultured cells were examined for alkaline phosphatase activity, stage specific embryo antigen 1 (SSEA-1) and for PAS reaction. A portion of the cultured cells was stained either with alkaline phosphatase substrate kit I or with Alkaline Phosphatase Chromogen (BCIP/NBT) kit (Biomeda Corporation, Foster City, USA) according to the manufacturer's instructions.

To evaluate the expression of SSEA-1 in the cultured cells, the cells were prepared as follows. First, a portion of the cultured cells were fixed for 20 min with Buin solution, then washed in PBS, and finally in distilled water. The cells were immersed in 0.3% hydrogen peroxide for 30 min, washed in distilled water, and then immersed in PBS for 5 min. The cells were then allowed to react overnight at 4°C with anti-SSEA-1 antibody, which had been diluted by a factor of 100 with PBS supplemented with 3% bovine serum albumin. The cells were washed in PBS and then finally stained with both VECTASTAIN ABC Kit (Vector Laboratories, Burlingame, USA) and DAB peroxidase substrate kit (Vector Laboratories) according to the manufacturer's instructions.

To examine the PAS reaction, a portion of the cultured cells was washed in distilled water, immersed for 5 min in 0.5% periodate at room temperature, and then washed again in distilled water. The cells were treated with Schiff's reagent for 5 min, immersed in sulfurous acid for 1 min at room temperature, and then washed in distilled water. These stained samples were observed using a light-field microscope, a Hoffman Modulation Contrast microscope, and a phase-contrast microscope.

RESULTS

FORTY-THREE FEMALE CYNOMOLGUS monkeys who were assumed to have ovulated were mated with a male, and eight became pregnant. Pregnancy diagnosis of the 43 females was determined based on measurement of the serum concentration of β-mCG and by ultrasonography (Table 1). Figure 1 shows photos of whole embryos extracted on day 30, 33 or 36 postovulation.

Figure 2 shows photos of the dorsal abdominal cavity after the removal of the entrails of embryos extracted on day 30, 33 or 36 postfertilization. In the embryo collected on day 30 postfertilization, the formation of gonads had not yet begun and no genital ridges were distinguishable. In the embryo at day 33 postfertilization, genital ridges had already formed next to the mesonephros. In the embryo at day 36 postfertilization, the gonads were clearly formed.

When cell clumps from the urogenital ridges and mesenteries of the embryo at day 30 postfertilization were cultured, only fibroblasts grew. Not only a fibroblast layer but also colonies composed of cells tightly

Table 1 Pregnancy diagnosis results

Pregnancy diagnosis using different methods		
β-mCG concentration	Ultrasonography	No. monkeys
+	+	8
+	–	0
–	+	0
–	–	35

β-mCG, beta subunit of macaque chorionic gonadotropin.

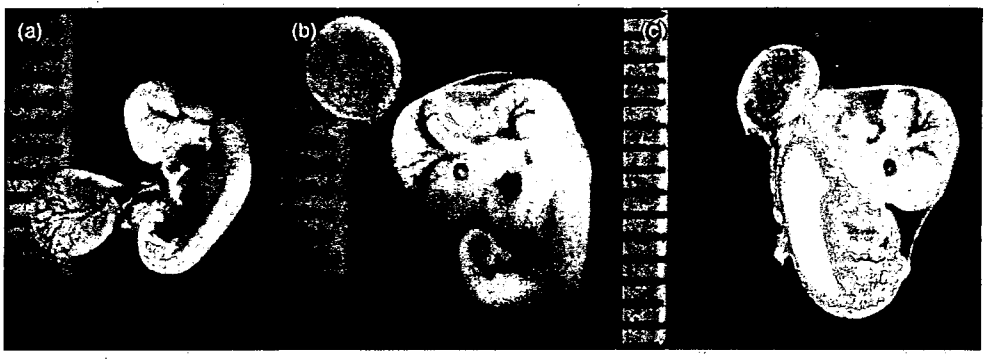

Figure 1 Photographs of embryos with allantois just after extraction from the uteruses of pregnant cynomolgus monkeys at days (a) 30 (b) 33 and (c) 36 postovulation. Scale bars at left are 1 mm apart.

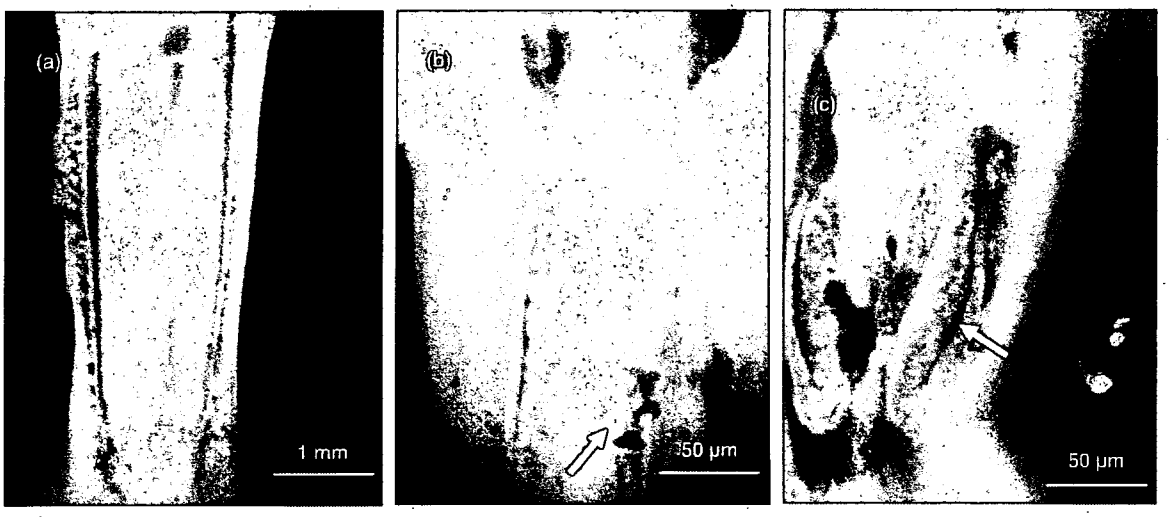

Figure 2 Photographs of the dorsal abdominal cavity of embryos after removal of the entrails. (a) Embryo at day 30 postfertilization. Formation of gonads has not started yet and the genital ridges are not yet distinguishable. (b) Embryo at day 33 postfertilization. Genital ridges (indicated by arrow) are next to the mesonephros. (c) Embryo at day 36 postfertilization. Arrow indicates clearly formed gonad.

bound to each other were formed from cell clumps collected from the hindguts. The cells comprising this colony were positive for both ALP activity and PAS reaction after culturing for 58 days (Fig. 3). Colonies and fibroblast layers also grew from cell clumps from the genital ridges and mesenteries of the embryo at day 33 postfertilization. The cells comprising these colonies were slightly positive for anti-SSEA-1 antibody, ALP activity, and were positive against PAS reaction after culturing for 33 days (Fig. 4). The PAS–hematoxylin-stained serial paraffin sections from the gonad that was clearly formed in the embryo at day 36 postfertilization showed the presence of PAS reaction positive cells. Live cells from this gonad after short-term culture were ALP activity positive (Fig. 5).

Cells that were enzymatically disaggregated into single cells from genital ridges and mesenteries of the embryo at day 33 postfertilization and cells that were cultured on a STO feeder layer in the presence of rhLIF, rhbFGF and forskolin were positive for ALP activity for 13 days (Fig. 6), although such cells could not be detected after the second passage (i.e. day 14 of culture). Cells cultured under these same conditions, but derived from gonads of the embryo at day 66 postfertilization, were positive for ALP activity up to day 56 of culture (eighth passage; Fig. 7).

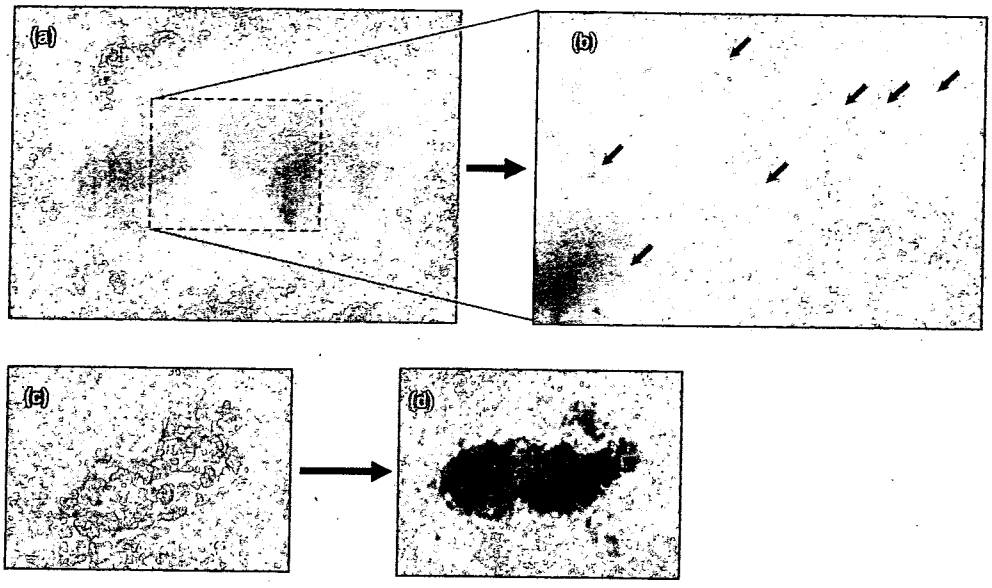

Figure 3 (a) Cultured cells from the genital ridges of a 30-day postfertilized embryo and (b) alkaline phosphatase (ALP) positive cells (indicated by the arrows) can be admitted. Colony before (c) and after (d) periodic acid Schiff (PAS) staining are indicated. The PAS stain is used for visualization of the polysaccharides because undifferentiated cells were often accumulated with the polysaccharide. The PAS-positive colony can be clearly seen in the photograph.

DISCUSSION

RADIORECEPTORASSAY RESULTS REPORTED by Yoshida *et al.* revealed that serum CG concentration in the early pregnancy of cynomolgus monkeys temporarily increases from days 21–28 after pregnancy, and then decreases to a low level, where it remains relatively constant.[5] Ogonuki *et al.* hypothesized that pregnancy in cynomolgus monkeys could be simply and conveniently diagnosed by measuring the serum β-mCG concentration using a commercially available EIA system for measuring serum β-hCG.[6] In the present study, as a first step in developing a system for estimating the differential potential of EG cells from cynomolgus monkeys we aimed at producing cynomolgus monkey embryos whose age at postfertilization was unambiguous, and at investigating the formation status of the gonads and the location of PGC. Our results verified that pregnancy diagnosis was possible by measuring the serum β-mCG concentration using an EIA system between weeks 3 and 4 postovulation. In an actual measurement using the EIA system, the serum β-mCG concentration of a pregnant female cynomolgus monkey was detectable at more than 100 ng/mL, but the serum β-mCG concentration of a non-pregnant monkey was below the detection limit. Pregnancy diagnosis using an EIA system and by ultrasonography gave the same result about the pregnancy status of all female monkeys used in this study. This demonstrates that an EIA system can be effectively used for early diagnosis of pregnancy in cynomolgus monkeys. Ogonuki *et al.* confirmed that ovulation can be assumed by monitoring the change in serum estrogen concentration using an EIA system before and after ovulation.[6] The postfertilization age of an embryo during early pregnancy can be accurately determined by combining the result measurement of estrogen and of β-mCG. When the collected embryo was directly observed using an optical microscope, the heartbeat was very slow and the actual development was approximately 2 days behind that based on the size of other embryos (data not shown). We concluded that this particular embryo showed abnormal development and, therefore, we did not use it for further study. Ultrasonography can help prevent unnecessary euthanasia in the future because abnormalities in embryos can be detected. In conclusion, ultrasonography should be used throughout the pregnancy, although pregnancy can be detected simply by measuring the β-mCG concentration during the early stages of pregnancy.

A cynomolgus monkey embryo grows as the embryonic age of postfertilization increases (Fig. 1). The formation

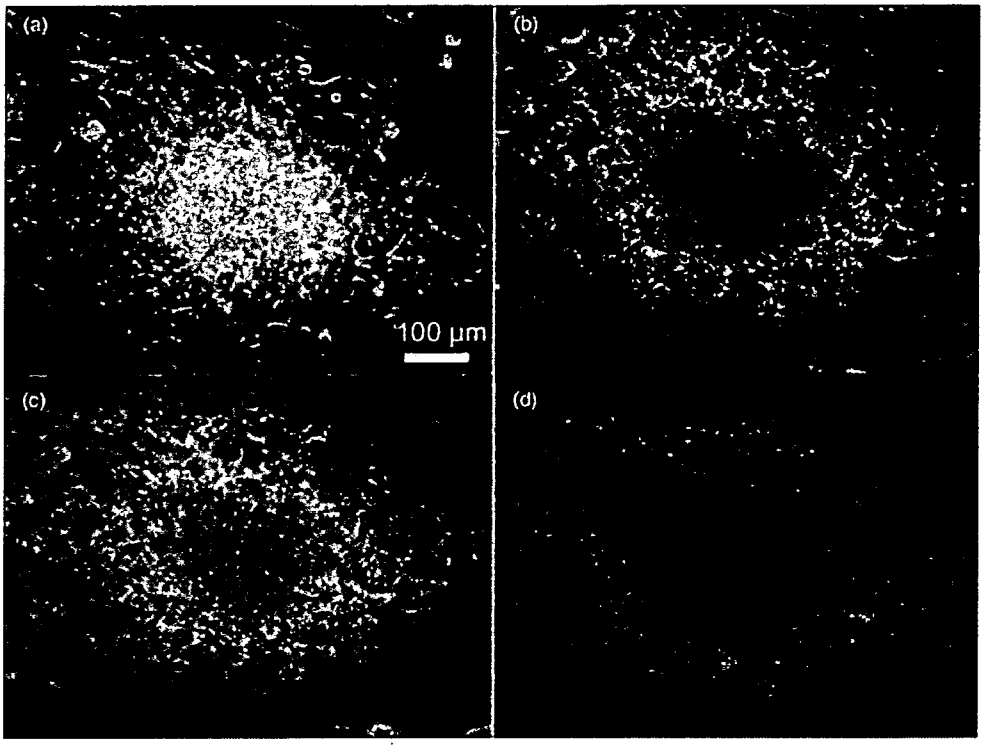

Figure 4 Phase-contrast microscope images of cell clumps from genital ridges and mesenteries of an embryo at day 33 postfertilization after 33 days of culture. (a) Cell clump before staining. Cells comprising these colonies were slightly positive for (b) anti-SSEA-1 antibody, (c) alkaline phosphatase activity, and were strongly positive for (d) periodic acid Schiff reaction.

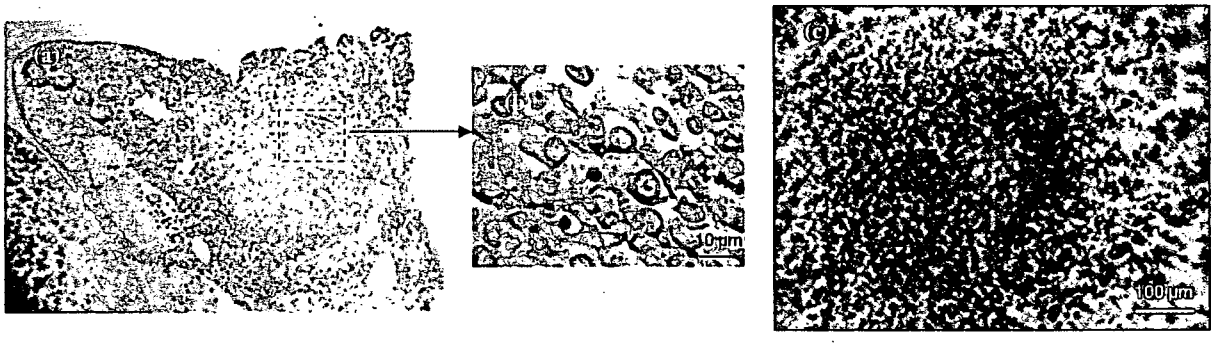

Figure 5 Photographs of serial paraffin sections of the gonad of an embryo at day 36 postovulation. (a) Low magnification and (b) high magnification images of a periodic acid Schiff (PAS)–hematoxylin stained sample. Some cells were positive for PAS reaction. (c) Alkaline phosphatase activity was positive after short-term culture of cells from the gonad.

status of the gonad in an embryo differed depending on the embryonic age of postfertilization. The genital ridges were not distinguishable at day 30 postfertilization, but started to form by day 33 postfertilization, and were clearly formed by day 36 postfertilization. Cynomolgus monkey PGC possibly migrate and colonize during this period between day 30 and 36 postfertilization. Direct observation of the location of PGC in a cynomolgus monkey embryo in this study indicated that PCG were in the hindguts at day 30 postfertilization,

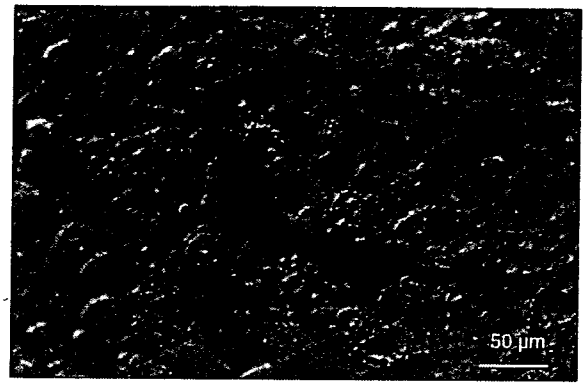

Figure 6 Hoffman modulation contrast image of a cell from the genital ridges and mesenteries of an embryo at day 33 postfertilization after 13 days of culture under conditions used to derive human embryonic germ cells. The cell (at center of photo) that was positive to alkaline phosphatase activity is stained red.

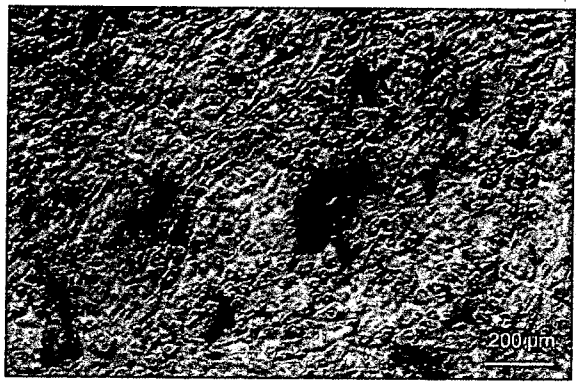

Figure 7 Hoffman modulation contrast image of a cell from the gonads of an embryo at day 66 postfertilization after 34 days of culture under conditions used to derive human embryonic germ cells. Cells that were positive to alkaline phosphatase activity are stained red.

arrived at the genital ridges via the mesenteries at approximately day 33 postfertilization, and finally colonized in the gonads by day 36 postfertilization. In mice, EG cells have been derived from PGC cultured from an embryo (aged between days 8.5 and 12.5 post coitus) under the presence of leukemia inhibitory factor, basic fibroblast growth factor and membrane-associated steel factor.[7,8] Based on our results about the formation status of the gonad and the location of PGC, the developmental stage of a cynomolgus monkey embryo at day 36 postfertilization apparently corresponds to that of a mouse embryo at day 12.5 post coitus (DPC). Stevens *et al.* reported that although more than 80% of mouse genital ridges at 12.5 DPC had the ability to form teratoma, this percentage dropped to approximately 8% at 13.5 DPC.[9] Labosky *et al.* reported that EG cells from a 12.5 DPC embryo did not have the ability to contribute to the germ line and that no EG cells could be derived from a 15.5 DPC embryo.[10] The PGC started meiosis at week 10 postconception in a human female embryo and in a rhesus monkey female embryo (same genus as cynomolgus monkey),[11] whereas PGC started meiosis at 13.5 DPC in a mouse female embryo. Although EG cell lines have been derived from 6 to 8-week postconception human embryos,[2,3] all cell lines were assumed to not have the ability to form teratoma. In conclusion, when the aim is to derive an EG cell line of a cynomolgus monkey, PGC should be collected from embryos earlier than day 33 postfertilization.

Genital ridges and mesenteries of a cynomolgus monkey embryo at day 33 postfertilization were cultured in this study according to the derivation and culture methods[2,3] of human EG cells. Namely, single cells to which the tissues were enzymatically dispersed were cultured on a STO feeder layer in culture medium supplemented with rhLIF, rhbFGF and forskolin. The cells were positive for ALP activity for a maximum of 13 days (Fig. 6). In contrast, cells cultured under the same conditions but derived from the gonads of an embryo at day 66 postfertilization were positive for ALP activity for 2 months (Fig. 7). This difference (i.e. the time that these PGC could be maintained by culture) is apparently related to the culture conditions and to the status of differentiation of PGC at collection. Derivation of an EG cell from a cynomolgus monkey was not achieved under the culture conditions used for humans. The PGC colonies obtained in the experiment disappeared with repeating passage. In the future, the successful derivation of EG cells will require research into the culture conditions or timing of passage for PGC from a cynomolgus monkey embryo collected earlier than day 33 postfertilization.

ACKNOWLEDGMENTS

THIS STUDY WAS supported in part by special coordination funds for the Promotion of Science and Technology and by a grant from the Ministry of Health, Labour and Welfare of Japan. We thank the staff responsible for the breeding program at the Corporation for Production and Research of Laboratory Primates for their technical assistance.

REFERENCES

[1] Asano T, Ageyama N, Takeuchi K *et al.* Engraftment and tumor formation after allogeneic in utero transplantation of primate embryonic stem cells. *Transplantation* 2003; 76: 1061–1067.

[2] Shamblott MJ, Axelman J, Wang S *et al.* Derivation of pluripotent stem cells from cultured human primordial germ cells. *Proc Natl Acad Sci USA* 1998; 95: 13726–13731.

[3] Tumpenny L, Brickwood S, Spalluto CM *et al.* Derivation of human embryonic germ cells: an alternative source of pluripotent stem cells. *Stem Cells* 2003; 21: 598–609.

[4] Honjo S. The Japanese tsukuba primate center for medical science (TPC): an outline. *J Med Primatol* 1985; 14: 75–89.

[5] Yoshida T, Suzuki K, Cho F, Honjo S. Serum chorionic gonadotropin levels determined by radioreceptorassay and early diagnosis of pregnancy in the cynomolgus monkey (*Macaca fascicularis*). *Am J Primatol* 1987; 12: 101–106.

[6] Ogonuki N, Tsuchiya H, Sankai T, Yoshida T, Cho F. Measurement of reproductive hormones in cynomolgus monkeys (*Macaca fascicularis*) using an enzyme immunoassay kit for human. In: *Proceedings of the Thirteenth International Congress of Comparative Endocrinology*. Yokohama, Japan, 1997: 883–886.

[7] Matsui Y, Zsebo K, Hogan BIM. Derivation of pluripotential embryonic stem cells from murine primordial germ cells in culture. *Cell* 1992; 70: 841–847.

[8] Resnick JL, Bixler LS, Cheng L, Donovan PJ. Long-term proliferation of mouse primordial germ cells in culture. *Nature* 1992; 359: 550–551.

[9] Stevens LC. Spontaneous and experimentally induced testicular teratomas in mice. *Cell Differ* 1984; 15: 69–74.

[10] Labosky PA, Barlow DP, Hogan BLM. Mouse embryonic germ (EG) cell lines transmission through the germline and differences in the methylation imprint of insulin-like growth factor 2 receptor (Igf2r) gene compared with stem (ES) cell lines. *Development* 1994; 120: 3197–3204.

[11] Wagenen GV, Simpson ME. *Embryology of the ovary and testis. Homo sapiens and Macaca mulatta*. New Haven: Yale University Press, 1965.